Numerical Modeling and Design of Single Photon Counter 4H-SiC Avalanche Photodiodes

Akin Akturk[†‡], Neil Goldsman[†‡]
[†] Department of Electrical and Computer Engineering
University of Maryland, College Park, MD, USA
[‡] CoolCAD Electronics
Takoma Park, MD, USA

Shahid Aslam[§], John Sigwarth[§], Fred Herrero[§]
[§] NASA Goddard Space Flight Center
Greenbelt, MD, USA

***Abstract*—We report device performance investigation of 4H-SiC avalanche photodiodes (APDs) with or without absorbing AlGaN cap layers, as 4H-SiCs' potential use in single photon counter APDs have drawn interest. Wide bandgap 4H-SiC photodiodes have low dark current levels at high temperatures and under intense radiation compared to silicon, and the 4H-SiC APDs are "solar blind" – transparent to the sun's visible spectrum. Additionally, they offer avalanche multiplications approaching a million, making single photon count possible. However, design and optimization of single photon counter APDs require a thorough understanding of impact ionization and optical absorption at the material level, and steady-state and transient APD operation at the device level. Here we address both of these levels.**

Keywords-avalanche photodiode; single photon counter; aluminum gallium nitride absorption layer; 4H-silicon carbide multiplication layer.

I. INTRODUCTION

To measure the temperature of the outer atmosphere, the space agency NASA requires the development of photo-detectors that can detect 9.2 eV photons that are emitted at the extremely low rate of 6 photons/sec using 400 by 100 micron^2 pixels. At 100% efficiency, this photon flux rate would correspond to a current of 6 electrons per second or approximately 10^{-18} Amps. To design such a high resolution detector, we use combined numerical modeling and experimental techniques. The numerical methods involve defining special boundary conditions to account for photon absorption near the semiconductor surface, as well as iteration methods to facilitate convergence during the massive generation of electron-hole pairs during the avalanche multiplication process. Furthermore, appropriate values of the ionization coefficients are extracted using theory and simulation to obtain agreement between numerical and experimental results.

Resolving a photon flux of 6 photons per second is virtually impossible at room temperature with a typical optical material such as GaAs because of the high dark current associated with its intrinsic carrier concentration. To detect such a small signal, we use wide bandgap semiconductors that have very small intrinsic carrier concentrations (theoretical values for their dark current are fifteen orders of magnitude lower than that of GaAs, and close to eighteen orders of magnitude lower than that of silicon). The key challenges here are to use modeling and characterization to design, to the fullest extent possible, a single photon detector to extract single photo-electrons, by using avalanche techniques, and to do so without increasing the dark current or noise level.

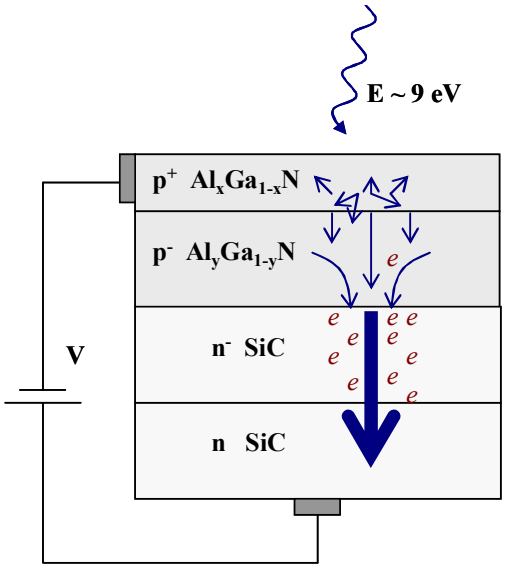

Figure 1. Our proposed photon detector struture with an aluminum gallium nitride (AlGaN) absorption layer and a 4H-silicon carbide (SiC) multiplication region for detecting low fluxes of 9 eV photons.

Ternary compounds that consist of column III nitrides have found numerous applications as building blocks of especially ultraviolet photodetectors. One such ternary compound is $Al_xGa_{1-x}N$, which is a semiconductor with a bandgap that can be tailored from 3.4 eV to 6.2 eV by changing the compound ratio x. These threshold energies that correspond to wavelengths ranging from 200 nm to 360 nm cover most of the near ultraviolet spectrum, and make AlGaN solar-blind. Therefore AlGaN photodetectors, which can be engineered to detect a wide range of frequencies, along with their inherent favorable material properties such as stability at high temperatures and under intense radiation, are devices of choice for detection at near ultraviolet spectrum.

978-1-4244-1753-7/08/$25.00 ©2008 IEEE

To increase the sensitivity of the AlGaN photodetector, an accompanying SiC avalanche diode is proposed as shown in Fig. 1. The ternary AlGaN crystal will absorb the incident photons and inject mobile carriers into an underlying carbide layer, which is epitaxially grown. This diode is reverse-biased, and it provides current multiplication via avalanche breakdown (largely in the carbide) to increase the number of photo-generated carriers. Even though a similar current multiplication using an AlGaN avalanche diode is possible, its prohibitive multiplication factors necessitate use of a material such as SiC. SiC avalanche diode may be engineered to provide multiplication factors a thousand times higher than that of the ternary AlGaN. Also, the bandgap of 4H-SiC, which is roughly 3.26 eV corresponding to 380 nm, is close to that of the ternary nitride. This fact might be used to minimize photon absorption at undesired wavelengths (the solar visible spectrum).

The key issue here is to create a layer structure capable of generating an avalanche effect at terminal biases that preclude breakdown, and thin enough to be grown without film fracture, spalling or excess crystal defect generation. Here we develop the theoretical underpinnings guiding our subsequent experimental work and fabrication.

An understanding of fundamental device physics is necessary for optimizing the AlGaN photodetector performance. To achieve this, we have developed a numerical-physical methodology for investigating single photon, extremely low dark current, AlGaN-SiC and 4H-SiC avalanche photodiodes (APDs) by building on our background work [1,2]. We have obtained agreement with experiments [3,4], showing avalanche multiplications approaching a million, making single photon count possible. Below we describe the physical and numerical techniques to achieve steady-state and transient APD operation.

II. Numerical Modeling

We first determine governing physics for the device operation. Then appropriate field dependent impact ionization rates and wavelength dependent absorption coefficients are obtained in conjunction with experiments and published data [3-5], as the device performance is very sensitive to these values. Next, we elaborate on the models employed for the device operation, ionization rates and optical generation.

A. AlGaN-SiC & 4H-SiC APD Physical-Mathematical Model and Challenges

To model the performances of AlGaN-SiC and 4H-SiC APD devices, we self-consistently solve the coupled semiconductor equations and the Poisson equation in conjunction with the details of optical generation, impact ionization, as well as the heterostructure valence and conduction band offsets.

$$\frac{\partial n}{\partial t} = \nabla.\left(-n\mu_n \nabla\phi + \mu_n V_{\text{th}} \nabla n\right) + G_t^n + G_{ii}^n + G_{op}^n \qquad (1)$$

$$\frac{\partial p}{\partial t} = \nabla.\left(p\mu_p \nabla\phi + \mu_p V_{\text{th}} \nabla p\right) + G_t^p + G_{ii}^p + G_{op}^p \qquad (2)$$

$$\nabla^2\phi = -\frac{q}{\varepsilon}\left(p - n + D\right) \qquad (3)$$

Above, we include the electron (1) and hole (2) current continuity equations along with the Poisson equation (3). Further, we introduce mobility μ, thermal voltage V_{th}, trap-assisted generation-recombination rate G_t, net ionized doping concentration D, dielectric constant ε, generation due to impact ionization G_{ii}, and optical generation G_{op}.

To obtain coupled device performance details of AlGaN photodetector and SiC avalanche diode under different illumination, temperature and bias conditions, we develop a mixed-mode simulator that can self-consistently resolve device operation. Specifically, different illumination levels at different wavelengths are given as input. Current or carrier count are provided as output, as a function of doping, bias, temperature and physical dimensions along with the potential profile and the carrier distribution. Later the output parameters are used to achieve the optimal parameters for maximizing quantum efficiency at 135 nm while minimizing sensitivity to visible photons, and staying compatible with standard epitaxial growth procedures for defect-free crystalline materials.

One of the challenges with the simulation of 4H-SiC devices is that the room temperature intrinsic carrier concentration (7×10^{-9} cm^{-3}) is low while the doping levels are comparable to those used for silicon. This requires resolving tens of orders of change in carrier concentrations. Also, under illumination the boundary conditions for electrons and holes deviate from those with thermal equilibrium or infinitely fast recombination times. At the boundaries non-equilibrium conditions that are proportional to the incident flux play an important role on the device operation. Another challenge is to resolve the effect of a single photo-electron within the context of the distributed transport-Poisson model, which is based on continuous partial-differential equations. Heterostructure band offsets are accounted for using spatially dependent intrinsic carrier concentrations and bands. The final key numerical challenge is to resolve the rapid transition from avalanche mode to breakdown and resistive operation. We develop numerical algorithms to overcome these problems.

B. 4H-SiC Electron-Hole Generation Rate due to Impact Ionization

To facilitate obtaining agreement with experiment, we incorporate the expressions for the hole (4) and electron (5) impact ionization rates per length written next for the crystal direction (0001) [5].

$$\alpha^p = \left(\frac{1}{\lambda^p}\right)\left(\frac{E}{E_i^p}\right)\exp\left[-\frac{E_i^p E_{op}^p}{E\left(E_{op}^p + E\right)}\right] \qquad (4)$$

$$\alpha^n = \left(\frac{1}{\lambda^n}\right)\left(\frac{E}{E_i^n}\right)\exp\left[-\frac{E_i^n E_{op}^n}{E^2}\right] \qquad (5)$$

Above α^n and α^p are electron- and hole-initiated (n for electrons, and p for holes) impact ionizations per length as a

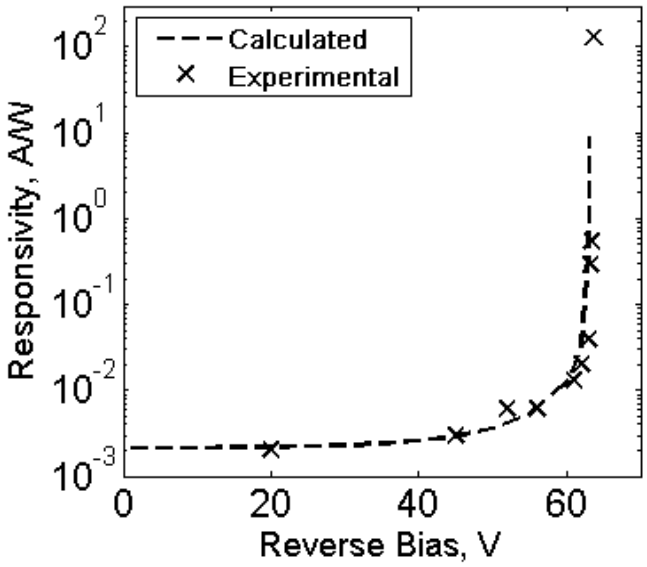

Figure 2. Calculated and experimental [3] responsivity of a 4H-SiC APD.

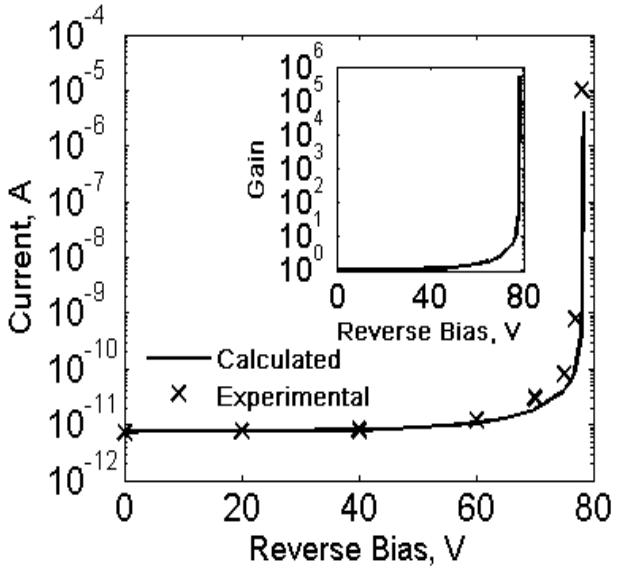

Figure 3. Calculated and experimental [4] current and gain of a 4H-SiC APD.

function of local electric field E ($=-\nabla\phi$). The mean free paths are approximately 3.0 nm ($=\lambda^n$) and 3.2 nm ($=\lambda^p$). In λ^n (λ^p), electrons (holes) can gain ionization energies of roughly 10eV (7eV) under E_i^n (E_i^p), which is the ionization field, and three times the optical phonon energy (=120 meV) under E_{op}^n (E_{op}^p). For 4H-SiC, the hole impact ionization rates are at least an order of magnitude larger than those of electrons for similar fields. Moreover, the resulting impact ionization rate is obtained as shown below by forming the product of α^n and α^p with the current densities, which are then inserted into the electron and hole continuity equations.

$$G_{ii}=\frac{1}{q}\left(\alpha^p J_p+\alpha^n J_n\right) \tag{6}$$

C. 4H-SiC Optical Absorption and Electron-Hole Generation Rate

To numerically calculate photocurrent due to an optical photon flux, we need the material absorption coefficient α_{op} [6] for a given wavelength, and its optical power reflectance from the surface. The latter affects the net photon flux that reaches the active device surface, and therefore the boundary conditions. The former optical parameter, which is the absorption coefficient, is important to obtain the spatial distribution of the optical electron-hole generation rate. This may greatly affect the calculated device performance, depending on whether the optical absorption is taking place near a dead layer or a depletion region. Using the absorption coefficient, optical electron-hole generation rate used in the APD device simulator is written as a function of distance r from the light entry point, as follows.

$$G_{op}=\left(\frac{\psi_{ph}}{A}\right)\alpha_{op}\exp\left(-\alpha_{op}r\right) \tag{7}$$

Here, ψ_{ph} is the number of photons that reach the active device surface per second; A is the active device area or effective area of impact. For experimental comparisons in Figs. 2-3, we take the wavelength of the incident photons as 320 nm, for which the absorption coefficient was experimentally determined to be approximately 2300 cm^{-1}. Furthermore, the absorption coefficient of AlGaN and 4H-SiC for a 9 eV photon are roughly 1×10^6 cm^{-1} and 2×10^6 cm^{-1}, respectively.

III. Comparison of Experimental and Calculated Results

To investigate different impact ionization rates and test the validity of our device, absorption and ionization models, we compared experimental results of [3] with those calculated using different impact ionization rates. For the p^+pn 4H-SiC APD with a doping profile described in [3], our calculated results (breakdown voltage, current gain and responsivity) matched well with those measured, as shown in Fig. 2. We determined the efficiency of that device as approximately 4%. We then examined another single photon counter APD [4]. After extracting the doping profile, we obtained good matches between experimental and calculated current and gain, as plotted in Fig. 3.

We next design an AlGaN-SiC APD with a cap p^+ AlGaN layer and an underlying n 4H-SiC. We take the ratio of AlN to GaN as 2/3 in the AlGaN ternary compound, and set the AlGaN absorption coefficient to a million per centimeter. Thickness of each layer is chosen such that it is longer than the depletion width that falls onto the corresponding layer. Here all absorption takes place in the AlGaN layer, and carrier

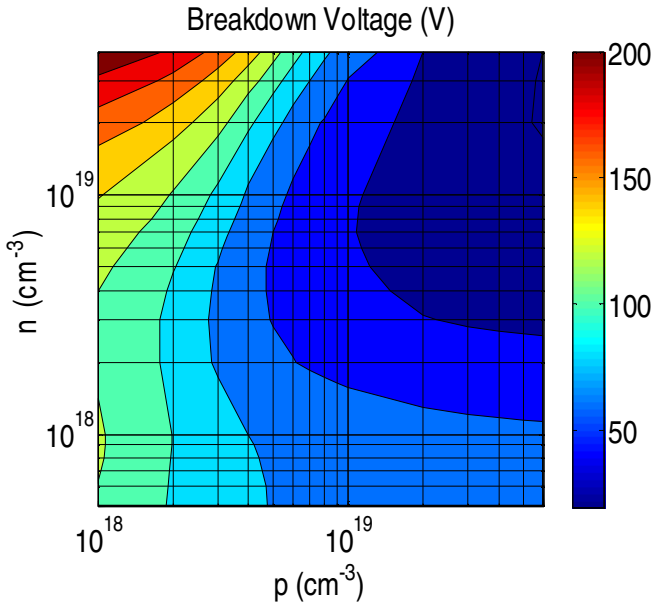

Figure 4. Breakdown voltage of an AlGaN-SiC APD as function of n (AlGaN) and p (SiC) side doping levels (or donor and acceptor concentrations).

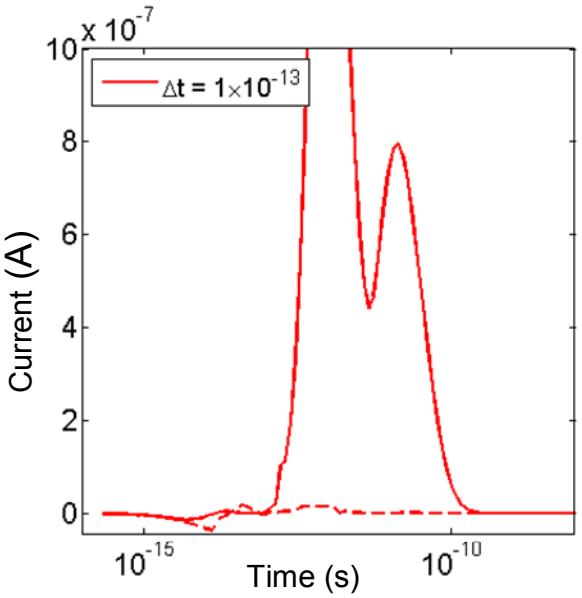

Figure 5. AlGaN-SiC APD's transient terminal current output at the SiC side to a single photon pulse hit at the AlGaN cap layer with a 0.1 ps duration. Dashed and solid lines are calculated currents when the impact ionization function is turned off and on, respectively.

amplification or multiplication occurs in the SiC region. In Fig. 4, we show the breakdown voltage for this APD as a function of the doping of the p and n sides. For cross sections taken at lower acceptor doping (p-side) levels, breakdown voltage slightly decreases as donor concentration increases, reaches a minimum and then rolls up to higher values. The breakdown voltage is high for low and high donor levels, reaching a minimum in between. For the former case built-in field values are low giving rise to reduced ionization rates, and for the high donor doping depletion width extends less into the n SiC region where the multiplication occurs. However, for an all 4H-SiC APD, as donor or acceptor concentration rise, the breakdown voltage falls due to higher built-in fields.

We also perform transient simulations to investigate transient responses of APDs to single photon hits, as measured in [4]. Fig. 5 shows the transient response of an APD we designed for breakdown at roughly 77.92 V to a single photon hit that is absorbed within one tenth of a picosecond. Here the overall amplification factor for the absorbed single photon is approximately a thousand, which is smaller than the multiplication factor that can be achieved under steady-state conditions for that chosen reverse bias voltage. However, due to the fast change of charge in time, a very high instantaneous current compared to the steady state case (roughly 10^{-18} Amps) is achieved. Also, our calculated current indicates that at the terminal we have two distinct current pulses first from zero to 0.1 ps due to the displacement current caused by the initial photon absorption, and second starting sometime after 0.1 ps to 0.1 ns due to the particle current as a result of the travelling pulse. For longer photon pulses (tens of picoseconds), the current pulses at the terminal due to the displacement and particle currents overlap, and they start separating as pulse duration decreases to a fraction of a picosecond.

IV. Conclusion

In conclusion, we developed a methodology to model novel AlGaN-SiC and 4H-SiC APDs, and obtained agreement with experiment, achieving numerical stability over more than six orders of magnitude variation of terminal current. Due to the low dark current levels, radiation-hardness, transparency to the solar spectrum, and stability at high temperatures associated with the wide bandgap 4H-SiC and AlGaN, such detectors can be employed to sense low photon fluxes in the ultraviolet range. In addition, high ionization rates of SiC can provide intrinsic amplification necessary for read-out circuitry.

References

[1] A. Akturk, N. Goldsman, N. Dhar, P. S. Wijewarnasuriya, "Modeling the temperature dependence and optical response of HgCdTe diodes", Proc. of ISDRS, pp. 70-71, 2005.

[2] A. Akturk, N. Goldsman, S. Aslam, J. Sigwarth, F. Herrero, "Comparison of 4h-sic impact ionization models using experiments and self-consistent simulations," to appear in Journal of Applied Physics, 2008.

[3] F. Yan, C. Qin, J. H. Zhao, M. Weiner, B. K. Ng, J. P. R. David, and R. C. Tozer, "Low-noise visible-blind UV avalanche photodiodes with edge terminated dy 2 degrees positive bevel", Electronics Lett., vol. 38(7), pp. 335-336, 2002.

[4] X. Xin, F. Yan, X. Sun, P. Alexandrove, C. M. Stahle, J. Hu, M. Matsumura, X. Li, M. Weiner, and H. J. Zhao, "Demonstration of 4H-SiC UV single photon counting avalanche photodiode", Electronics Lett., vol. 41(4), pp. 212-214, 2005.

[5] A. O. Konstantinov, Q. Wahab, N. Nordell, and U. Lindefelt, "Ionization rates and critical fields in 4H silicon carbide", Appl. Phys. Lett., vol. 71(1), pp. 90-92, 1997.

[6] Z. Dilli, N. Goldsman, M. Peckerar, A. Akturk, and G. Metze, "Design and testing of a self-powered 3D integrated SOI CMOS system", Microelectronic Eng., vol. 85, pp. 388-394, 2008.